UC Irvine
UC Irvine Previously Published Works

Title

Bedforms as Biocatalytic Filters: A Pumping and Streamline Segregation Model for Nitrate Removal in Permeable Sediments

Permalink

https://escholarship.org/uc/item/9112p1xz

Journal

Environmental Science and Technology, 49(18)

ISSN

0013-936X

Authors

Azizian, Morvarid
Grant, Stanley B
Kessler, Adam J
et al.

Publication Date

2015-09-15

DOI

10.1021/acs.est.5b01941

Peer reviewed

Bedforms as Biocatalytic Filters: A Pumping and Streamline Segregation Model for Nitrate Removal in Permeable Sediments

Morvarid Azizian,[†] Stanley B. Grant,*[,†,‡,§] Adam J. Kessler,[∥] Perran L. M. Cook,[∥] Megan A. Rippy,[‡] and Michael J. Stewardson[§]

[†]Department of Chemical Engineering and Materials Science and [‡]Department of Civil and Environmental Engineering, Henry Samueli School of Engineering, University of California, Irvine, California 92697, United States

[§]Department of Infrastructure Engineering, Melbourne School of Engineering, The University of Melbourne, Melbourne, Victoria 3010, Australia

[∥]Water Studies Centre, School of Chemistry, Monash University, Clayton 3800, Australia

S Supporting Information

ABSTRACT: Bedforms are a focal point of carbon and nitrogen cycling in streams and coastal marine ecosystems. In this paper, we develop and test a mechanistic model, the "pumping and streamline segregation" or PASS model, for nitrate removal in bedforms. The PASS model dramatically reduces computational overhead associated with modeling nitrogen transformations in bedforms and reproduces (within a factor of 2 or better) previously published measurements and models of biogeochemical reaction rates, benthic fluxes, and in-sediment nutrient and oxygen concentrations. Application of the PASS model to a diverse set of marine and freshwater environments indicates that (1) physical controls on nitrate removal in a bedform include the pore water flushing rate, residence time distribution, and relative rates of respiration and transport (as represented by the Damkohler number); (2) the biogeochemical pathway for nitrate removal is an environment-specific combination of direct denitrification of stream nitrate and coupled nitrification-denitrification of stream and/or sediment ammonium; and (3) permeable sediments are almost always a net source of dissolved inorganic nitrogen. The PASS model also provides a mechanistic explanation for previously published empirical correlations showing denitrification velocity (N_2 flux divided by nitrate concentration) declines as a power law of nitrate concentration in a stream (Mulholland et al. *Nature*, 2008, *452*, 202−205).
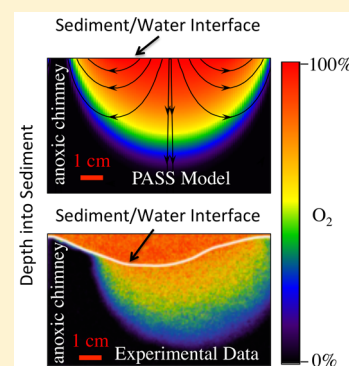
INTRODUCTION

Permeable sediments line the bottom of rivers and marine coastlines worldwide. The movement of water, heat, and mass through permeable sediments is a key component of many globally important ecosystem services, including the provision of benthic habitats,[1−3] pollutant attenuation,[4,5] and biogeochemical cycling.[6−8] In the highly productive inner shelf region of the world's oceans, permeable sands are responsible for 24−73% of benthic respiration and 15% of denitrification.[9] On land, the fate of 75% of nitrogen added by agricultural activities is unaccounted for,[10,11] and much of the missing nitrogen is thought to be denitrified within permeable stream sediments.[12] Permeable sediments can also serve as sources or sinks for phosphorus,[5,12−14] heavy metals,[4,5] fecal indicator bacteria,[15,16] and human pathogens.[17,18]

The profound influence permeable sediments exert on global biogeochemical cycling and regional water quality can be attributed to[9,19−22] (1) the transport of mass and heat across the sediment−water interface by physical and biological processes and (2) the presence of microbial communities in the sediments that catalyze oxidation−reduction reactions. As noted in a recent review article, these two features transform permeable sediments into highly reactive biocatalytic filters.[9] Here we present a simple mechanistic model for the biocatalytic transformation of nitrate by permeable sediments in marine and freshwater systems. The paper is organized as follows. We begin with a description of the modeling framework adopted in this study and then evaluate the model in light of (1) previously published experimental measurements, (2) previously published numerical simulations, and (3) relaxation of one of the model's key assumptions. The model is then used to identify physical and biocatalytic controls on nitrate removal in six environments (three coastal marine and three terrestrial streams) and to evaluate a previously published empirical correlation for the uptake velocity of nitrate in streams.

■ ADVECTIVE PUMPING MODEL (APM) FOR FLOW-TOPOGRAPHY PORE WATER EXCHANGE

As water flows over the top of a bedform, dynamic pressure variations along the sediment−water interface arise due to acceleration and deceleration of the flow and boundary layer separation.[20−25] These dynamic pressure variations pump water, oxygen, and nutrients into the sediment in high-pressure regions (downwelling zones) and out of the sediment in low-pressure regions (upwelling zones). Here we adopt an idealized model of this pumping process (called the advective pumping model or APM) first proposed and experimentally validated by Elliott and Brooks.[26,27] In the APM, the variation in dynamic pressure is mimicked with an assumed sinusoidal pressure variation over a flat sediment−water interface (Figure 1A). Of
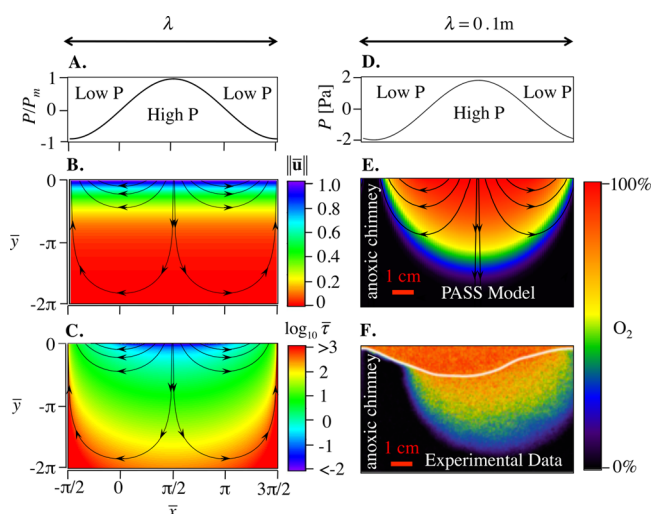
Figure 1. Features of the APM velocity field (A−C) and an experimental test of the PASS model (D−F). The APM assumes flow across the sediment−water interface is driven by a sinuosoidal pressure variation over a flat sediment bed (A). This pressure variation drives flow into the sediment in high pressure regions (downwelling zones) and out of the sediment in low pressure regions (upwelling zones) (B). Water parcels moving through the sediment experience a diverse range of streamline trajectories and ages (C). The PASS model was used to simulate the reactive transport of oxygen through a sandy ripple with a 10 cm wavelength (D). The pore fluid concentrations of oxygen predicted by the PASS model (E) are qualitatively similar to oxygen measurements with a two-dimensional planar optode (see main text) (F). Variables appearing in this figure include bedform wavelength (λ); pressure (P) and maximum pressure (P_m) at the sediment−water interface; reduced horizontal ($\bar{x}$) and vertical ($\bar{y}$) coordinates (depth into the sediment bed corresponds to $\bar{y} < 0$); absolute magnitude of the reduced pore fluid velocity $\|\bar{\mathbf{u}}\| = \|\mathbf{u}\|/(\pi k_m)$ where k_m is the pore-water flushing rate; and a reduced form of the water parcel age $\bar{\tau} = \tau/\tau_T$. The five streamlines shown in panels B, C, and E were chosen so that the volume of water (per unit width of stream) flowing between any two adjacent streamlines is the same and equal to 1.7 L/m/day (see the Supporting Information).

course, real bedforms are not flat and the dynamic pressure variation over a bedform is not purely sinusoidal.[28] Nevertheless, the flow field predicted by the APM is qualitatively similar to experimental and computational observations of pore fluid flow fields induced by stream−bedform interactions[26,28,29] and reproduces to within 11% computational estimates of benthic water flux[30] (the APM stream function, from which the x- and y-components of the two-dimensional velocity field can

be calculated, is presented in the Supporting Information). Given its simplicity and consistency with experimental observations and numerical simulations, the APM is an excellent starting point for the modeling described next.

■ APM WATER PARCEL AGE AND RESIDENCE TIME DISTRIBUTION (RTD)

If permeable bedforms are biocatalytic filters then it stands to reason that methods developed for the design and analysis of chemical reactors may prove useful. A critical feature of any chemical reactor is the time water parcels spend in the reactor.[31] Here we define two such transport time scales: water parcel age and residence time distribution.

Water Parcel Age. The water parcel age $\tau(\bar{x},\bar{y})$ is the time a water parcel spends traveling from where it first crosses into the sediment in a downwelling zone to any location $(\bar{x},\bar{y})$ in the sediment. Here, the variables $\bar{x} = 2\pi x/\lambda$ and $\bar{y} = 2\pi y/\lambda$ are reduced forms of the horizontal and vertical coordinates x and y, respectively, where λ represents the wavelength of the sinusoidal pressure variation (assumed equal to the wavelength of a bedform) (Figure 1A). Several points should be kept in mind. First, the APM flow field is steady-state, stream-wise periodic, and two-dimensional. Consequently, any location $(\bar{x},\bar{y})$ in the sediment is associated with a single streamline and a single value for the water parcel age. Second, all downwelling zones in the APM are identical or mirror image (e.g., compare the one located for $\bar{x}$ values between $0 \leq \bar{x} \leq \pi/2$ and its mirror image located for $\bar{x}$ values between $\pi/2 \leq x \leq \pi$, Figure 1B). Thus, without loss of generality we can calculate the age of water parcels that transit from one downwelling zone ($0 \leq x \leq \pi/2$) to an adjacent upwelling zone ($-\pi/2 \leq x \leq 0$) (Figure 1B). An explicit formula for the age of water parcels entering this particular downwelling zone (and by inference all downwelling zones) can be derived from the APM (see the Supporting Information):

$$\bar{\tau}(\bar{x}, \bar{y}) = \frac{\tau(\bar{x}, \bar{y})}{\tau_T} = \frac{\cos^{-1}(e^{\bar{y}}\cos\bar{x}) - \bar{x}}{2e^{\bar{y}}\cos\bar{x}}, \quad \bar{y} \leq 0,$$
$$-\pi/2 \leq \bar{x} \leq \pi/2 \tag{1a}$$

$$\tau_T = \lambda\theta/\pi^2 k_m \tag{1b}$$

The parameter τ_T is a characteristic time scale for transport through a bedform. It can be interpreted as the time it would take a water parcel to travel the distance λ while moving at speed k_m/θ, where k_m is the volume of water flowing through the bedform per unit area of bed surface ($m^3\ s^{-1}\ m^{-2}$) (also called the Darcy flux,[32] pore−water flushing rate,[9] downwelling velocity,[30] and mass-transfer coefficient[30]) and θ (−) is sediment porosity (the π^2 appearing in the denominator of eq 1b is included for mathematical convenience). For the duration of this paper, we refer to k_m as the pore−water flushing rate. The pore−water flushing rate can be measured in the field,[33] in laboratory flumes,[30] or calculated from eq 2 based on bedform geometry (wavelength λ (m) and height Δ (m)), hydraulic conductivity of the sediment (K_h (m s^{-1})), streamflow velocity (U (m s^{-1})), and stream depth (H (m)).[26,27]

$$k_m = 0.28\frac{K_h U^2}{g\lambda}\left(\frac{\Delta/H}{0.34}\right)^\gamma, \quad \gamma = \begin{cases} 3/8 & \text{for } \Delta/H < 0.34 \\ 3/2 & \text{for } \Delta/H \geq 0.34 \end{cases}$$
$$\tag{2}$$

Water parcel ages predicted by eq 1a vary more than 5 orders of magnitude (Figure 1C). Some water parcels move quickly along short streamlines located near the surface ($\overline{\tau}$ < 0.1, dark blue to purple colors in Figure 1C), while others travel slowly along long streamlines that penetrate deep into the sediment ($\overline{\tau}$ > 100, yellow to red colors).

Residence Time Distribution. The residence time distribution (RTD) function $F_{RTD}(\tau_f)$ is defined as the fraction of water volume cycling through a bedform with final age τ_f or younger upon exiting. The RTD takes into account both the age of water parcels exiting the sediments and the partitioning of water flux across streamlines.[31] The distinction between $\tau(\overline{x},\overline{y})$ and τ_f is the former represents the age of the water parcel at any location in the sediment (see eq 1a) while the latter represents the final age of a water parcel leaving the sediment bed. The final age τ_f varies by where a streamline intersects the x-axis (at $y = 0$) in a downwelling zone. We denote this intersection point as $x = x_0$, which in reduced form becomes $\overline{x} = \overline{x}_0$ where $\overline{x}_0 = 2\pi x_0/\lambda$. Given these definitions, an RTD can be derived for the same downwelling zone analyzed above (and by inference all downwelling zones, see the Supporting Information):
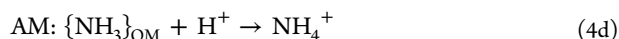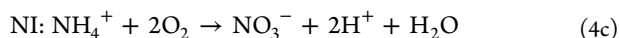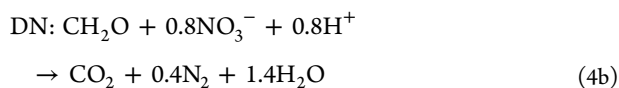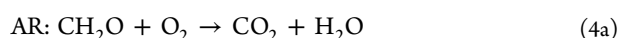
$$F_{RTD}(\overline{\tau}_f) = 1 - \cos[\overline{x}_0(\overline{\tau}_f)], \quad 0 \leq \overline{x}_0 \leq \pi/2 \tag{3a}$$

$$\overline{\tau}_f \equiv \frac{\tau_f}{\tau_T} = \frac{\overline{x}_0}{\cos \overline{x}_0}, \quad 0 \leq \overline{x}_0 \leq \pi/2 \tag{3b}$$

Equation 3b is an implicit form of the function $\overline{x}_0(\overline{\tau}_f)$; i.e., for any choice of the final age $\overline{\tau}_f$, the equation can be solved to find the corresponding value of $\overline{x}_0$, which can then be substituted into eq 3a to yield a value for F_{RTD}. Consistent with the diversity of streamline trajectories shown in Figure 1C, the RTD exhibits a broad (logarithmic) range of final ages (Figure S1, Supporting Information). The RTD derived here (eqs 3a and 3b) is mathematically equivalent to the residence time expression derived for the APM by Elliott and Brooks[26] (see the Supporting Information).

PUMPING AND SEGREGATED STREAMLINE (PASS) MODEL FOR NITRATE

In this paper, we combine the APM flow field with biogeochemical reactions for aerobic respiration (AR), nitrification (NI), denitrification (DN), and ammonification (AM).[34]

$$\text{AR: } CH_2O + O_2 \rightarrow CO_2 + H_2O \tag{4a}$$

$$\text{DN: } CH_2O + 0.8NO_3^- + 0.8H^+$$
$$\rightarrow CO_2 + 0.4N_2 + 1.4H_2O \tag{4b}$$

$$\text{NI: } NH_4^+ + 2O_2 \rightarrow NO_3^- + 2H^+ + H_2O \tag{4c}$$

$$\text{AM: } \{NH_3\}_{OM} + H^+ \rightarrow NH_4^+ \tag{4d}$$

The notation $\{NH_3\}_{OM}$ in eq 4d refers to the generation of ammonium by the microbial respiration of sediment organic matter.

The APM assumes that flow through a bedform is laminar. Under laminar flow, it can often be assumed that water parcels do not mix with adjacent water parcels as they travel through the reactor,[31,35] although this assumption may breakdown in heterogeneous bedform sediments (discussed later).[36] As applied to bedforms, this "segregated streamline hypothesis"

implies that molecular diffusion and mechanical dispersion can be neglected, and therefore, the steady-state concentrations of oxygen (C_{O_2}), ammonium ($C_{NH_4^+}$), and nitrate ($C_{NO_3^-}$) along any streamline through the sediment will evolve with water parcel age (τ) according to the following set of mass balance expressions:[32,35,37]

$$\frac{dC_{O_2}}{d\tau} = -R_{AR} - 2R_{NI} \tag{5a}$$

$$\frac{dC_{NO_3^-}}{d\tau} = R_{NI} - R_{DN} \tag{5b}$$

$$\frac{dC_{NH_4^+}}{d\tau} = R_{AM} - R_{NI} \tag{5c}$$

Monod rate expressions (based on a consensus evaluation of field and laboratory data[34]) were adopted for the rates of aerobic respiration (R_{AR}), ammonification (R_{AM}), nitrification (R_{NI}), and denitrification (R_{DN}):

$$R_{AR} = \frac{R_{min}C_{O_2}}{C_{O_2} + K_{O_2}^{sat}} \tag{6a}$$

$$R_{AM} = \frac{1}{\gamma_{CN}}R_{min} \tag{6b}$$

$$R_{NI} = k_{NI}C_{O_2}C_{NH_4^+} \tag{6c}$$

$$R_{DN} = \theta_{O_2}^{inh}\kappa\frac{R_{min}C_{NO_3^-}}{C_{NO_3^-} + K_{NO_3^-}^{sat}}; \quad \theta_{O_2}^{inh} = \frac{K_{O_2}^{inh}}{C_{O_2} + K_{O_2}^{inh}} \tag{6d}$$

Parameters appearing here include the respiration rate of sediment organic matter (R_{min} (mol m^{-3} s^{-1})), a constant for ammonification (γ_{CN} (−)), a bimolecular nitrification rate constant (k_{NI} (m^3 mol^{-1} s^{-1})), half-saturation constants for aerobic respiration ($K_{O_2}^{sat}$ (mol m^{-3})), denitrification ($K_{NO_3^-}^{sat}$ (mol m^{-3})), and oxygen inhibition ($K_{O_2}^{inh}$ (mol m^{-3})), and an empirical factor $\kappa = 0.05$ (−).

Combining eqs 5a through 6d, we arrive at three ordinary differential equations (equations S12a−S12c, Supporting Information) that can be numerically integrated to yield the chemical evolution of a water parcel as it moves along a streamline through the sediment:

$$\overline{C}_i(\overline{\tau}_R; \text{chemistry}) \equiv \frac{C_i(\overline{\tau}_R; \text{chemistry})}{C_{O_2}(0)} \tag{7a}$$

$$\overline{\tau}_R \equiv \frac{\tau(\overline{x}, \overline{y})}{\tau_R} \tag{7b}$$

$$\tau_R = \frac{K_{O_2}^{sat}}{R_{min}} \tag{7c}$$

Here, C_i (mol m^{-3}) represents the pore fluid concentration of the ith chemical species (oxygen, nitrate, or ammonium), $\overline{\tau}_R$ is the reduced age of the water parcel, $C_{O_2}(0)$ (mol m^{-3}) is the in-stream concentration of oxygen, and τ_R (s) is a time scale for the respiration of sediment organic matter. Conceptually, reduced age is a nondimensional quantity that represents the time a water parcel travels through the sediment normalized by the characteristic time scale associated with aerobic respiration

Table 1. Benthic Fluxes, Average Rates of Production (>0) or Consumption (<0) of Oxygen, Nitrate, and Ammonium in the Sediment (P_{avg}), and Average Rates of Aerobic Respiration, Nitrification, Denitrification, and Ammonification in the Sediment (R_{avg}) Calculated from the PASS Model, Kessler Numerical Flume Studies, and COMSOL Simulations in Which the Segregated Streamline Hypothesis (or SSH) Is Relaxed[a]

	flux (mol m^{-2} s^{-1}) × 10^8			P_{avg} (mol m^{-3} s^{-1}) × 10^7			R_{avg}[b] (mol m^{-3} s^{-1}) × 10^7			
	O_2	NO_3^-	NH_4^+	O_2	NO_3^-	NH_4^+	AR	NI	DN	AM
PASS	−23	−0.32	5.2	−65	−0.93	15	63	1.3	2.3	16
Kessler et al.	−14	−0.39	4.2	−50	−1.4	15	48	1.0	2.5	16
COMSOL	−23	−0.06	4.9	−65	−0.18	14	62	1.8	2.0	16

[a]Positive (negative) flux values correspond to net transport out of (into) the sediment bed. [b]AR = aerobic respiration; NI = nitrification; DN = denitrification; AM = ammonification.

of organic matter in the sediment. The word "chemistry" in eq 7a is shorthand for the seven reduced parameters that collectively define in-stream concentrations and reaction rates including: (1) the relative rates of nitrification and aerobic mineralization ($\delta \equiv k_{NI}C_{O_2}(0)/(R_{min}/K_{O_2}^{sat})$); (2) normalized saturation constants for oxygen ($\bar{K}_{O_2}^{sat} \equiv K_{O_2}^{sat}/C_{O_2}(0)$), nitrate ($\bar{K}_{NO_3^-}^{sat} \equiv K_{NO_3^-}^{sat}/C_{O_2}(0)$), and oxygen inhibition of denitrification ($\bar{K}_{O_2}^{inh} \equiv K_{O_2}^{inh}/C_{O_2}(0)$); (3) normalized stream concentrations of ammonium ($\alpha \equiv C_{NH_4^+}(0)/C_{O_2}(0)$) and nitrate ($\beta \equiv C_{NO_3^-}(0)/C_{O_2}(0)$); and (4) net mineralization of carbon relative to production of ammonium (γ_{CN}) (top seven rows of Table S1).

When eq 7a is combined with the APM solution for water parcel age ($\bar{\tau}(\bar{x},\bar{y})$, eq 1a) we arrive at a solution for the pore fluid concentrations of oxygen and nutrients from which all other parameters of interest (e.g., benthic flux, average reaction rates, and uptake velocities, see later) can be calculated:

$$\frac{C_i(\bar{x}, \bar{y}; \textbf{chemistry})}{C_{O_2}(0)} = \bar{C}_i(\bar{\tau}_R = \textbf{Da}\bar{\tau}(\bar{x}, \bar{y}); \textbf{chemistry}) \tag{8a}$$

$$\textbf{Da} = \frac{\tau_T}{\tau_R} \tag{8b}$$

The Damkohler number (**Da**) is defined as the ratio of time scales for transport (τ_T, eq 1b) and respiration of sediment organic matter (τ_R, eq 7b); it can also be interpreted as the relative rate of respiration and transport within the bedform. Note that our definition of the Damkohler number differs from that presented in a similar study by Zarnetske et al.[38] Specifically, our definition of **Da** is fixed by the values of τ_T and τ_R (corresponding to specific choices of the RTD of water parcels and respiration rate in the sediment, respectively), while Zarnetske et al.'s definition varies continuously along any streamline through the sediment. As will be shown later, by adopting eq 8b as the definition of **Da**, this nondimensional parameter becomes a controlling variable for the net flux of nitrate across the sediment-water interface over a wide spectrum of aquatic environments. Because our model relies on both the APM and the streamline segregation hypothesis (SSH), we refer to it as the pumping and streamline segregation (PASS) model.

TESTING THE PASS MODEL

The PASS model is derived from a number of assumptions that individually or collectively may render it unsatisfactory in practice. To address this concern, we compared the PASS model with (1) O_2 measurements in an experimental flume; (2)

concentrations and fluxes predicted by an experimentally validated flow and reactive transport model; and (3) a numerical simulation in which the SSH was relaxed.

Comparison with O_2 Measurements. As a first test, the PASS model was compared to oxygen measurements reported in a study of nitrogen cycling in sandy marine sediments by Kessler et al.[39] The experimental setup involved a recirculating flume to which sediment (from Port Phillip Bay, Melbourne, Australia) was added and artificially sculpted into ripples of height ∼1 cm and wavelength ∼10 cm. Water collected from the same field site was circulated through the flume at a depth and average flow velocity of approximately 13 cm and 16 cm s^{-1}, respectively. From the set of parameter values reported by Kessler (Table S2, Supporting Information) we estimate a pore water flushing rate (from eq 2) of $k_m = 1.64 \times 10^{-6}$ m s^{-1}, a characteristic travel time through a single ripple (from eq 1b) of $\tau_T = 36$ min, and a sinusoidal pressure amplitude at the sediment–water interface of approximately 2 Pa (using a rearranged form of eq 2g in ref 30, Figure 1D). Kessler also reported in-stream nutrient concentrations and rate constants needed to calculate values for the seven reduced parameters in Table S1 (first column). From these data, we estimate a respiration time scale of $\tau_R = K_{O_2}^{sat}/R_{min} = 23$ min. Thus, oxygen consumption in the bedform is likely to be both reaction and transport controlled (i.e., the relative rate of respiration and transport is approximately unity, $\textbf{Da} = \tau_T/\tau_R = 1.6$). Indeed, pore fluid oxygen concentrations predicted by the PASS model (Figure 1E) indicate that the reaction field is strongly influenced by the flow field: oxygen saturated waters penetrate to a depth of ∼4 cm in the downwelling zone, and an "anoxic chimney" extends to the surface in the upwelling zone. These PASS predictions are qualitatively similar to measured two-dimensional profiles of oxygen saturation beneath a single ripple in Kessler's flume experiments (obtained with a 2D planar optode, Figure 1F).[39] While the experimental and model results are similar, there are two noteworthy differences. First, the concentration gradient along the edge of the aerobic zone is steeper in the PASS model than in the experimental study. Second, the areal extent of the aerobic zone appears smaller in the experimental study (taking into account the undulating nature of the ripple surface, as denoted by the white curve in Figure 1F). The first difference is a consequence of neglecting molecular diffusion and mechanical dispersion, while the latter difference reflects the PASS model's oversimplification of mass transfer across the sediment–water interface (i.e., flat sediment–water interface and a simplified velocity field). These two limitations are explored in more detail below.

Comparison with Numerical Flume Studies. Kessler also presented "numerical flume" studies in which the pore fluid

concentrations of oxygen, nitrate, and ammonium beneath a single ripple were calculated using an experimentally calibrated flow and reactive transport model[39,40] (see the Supporting Information, Figure S3, Table S2). Pore fluid concentrations calculated from the PASS model are qualitatively similar to Kessler's numerical flume results except that (Figure S4, Supporting Information): (1) the PASS model predicts symmetrical concentration fields (consistent with the APM's symmetric velocity field), while the numerical flume predicts asymmetrical concentration fields (reflecting the more realistic pore fluid velocity field generated by turbulent streamflow over a ripple); and (2) the PASS model has a larger aerobic zone compared to the numerical flume prediction (consistent with the 2D planar optode measurements discussed above). The PASS model approximately reproduces Kessler's predictions for: (1) locations of reaction zones in the sediment (aerobic respiration, nitrification, denitrification: Figure S5, Supporting Information); (2) where in the sediment oxygen, nitrate, and ammonium are produced or consumed (Figure S6, Supporting Information); (3) benthic flux of nitrate and ammonium, although the benthic flux of oxygen is somewhat overestimated (relative differences of 18%, 24%, and 64%, Table 1); (4) average rates for the production or consumption of oxygen, nitrate, and ammonium in the sediment (relative differences of 30%, 34%, and 0%, Table 1); and (5) average rates for respiration, nitrification, and denitrification in the sediment (relative differences of 31%, 30%, and 8%, Table 1). In summary, the PASS model reproduces (within 35% or better) Kessler et al.'s estimates of biogeochemical reactions rates and benthic fluxes, with the exception of the benthic flux of oxygen which is overestimated by 64%. As will be shown in the following sections, the model's overestimation of benthic oxygen flux probably stems from assuming that the sediment-water interface is flat and the hyporheic exchange flow-field is symmetrical.

Evaluating the Segregated Streamline Hypothesis (SSH). As a final test, we conducted a numerical simulation (using COMSOL Multiphysics (version 4.4), see the Supporting Information for details) in which the SSH was relaxed (i.e., water parcels were allowed to mix across streamlines by molecular diffusion and mechanical dispersion), but all other aspects of the PASS model were retained (flat sediment–water interface, the APM velocity field, and reaction rate laws described above). Comparing benthic fluxes predicted by the PASS and COMSOL models (first three columns in Table 1) we find that relaxing the SSH causes: (1) no change in the benthic flux of oxygen (relative difference of 0%); (2) a large reduction in the flux of nitrate into the sediment (relative difference of 81%); and (3) a small reduction in the flux of ammonium out of the sediment (relative difference of 6%). These results can be explained by the role of molecular diffusion and mechanical dispersion in delivering oxygen to anoxic regions of the sediment. In particular, when the SSH is relaxed more oxygen is delivered to the anoxic chimney which, in turn, increases the average rate of nitrification, decreases the average rate of denitrification, and thereby reduces the net flux of nitrate across the sediment-water interface (see difference plots in Figure S7, Supporting Information, and average nitrification and denitrification rates for the PASS and COMSOL models in Table 1). By contrast, relaxing the SSH has no effect on the benthic flux of oxygen because mass transport across the sediment—water interface is dominated by advection. Remarkably, when benchmarked relative to Kessler's

numerical flume experiment, relaxing the SSH increases the nitrate flux error from 18% (for the PASS model) to 64% (for the COMSOL model) (Table 1). This surprising result can be explained by a fortuitous canceling of errors: the PASS model overestimates the flux of oxygen across the sediment—water interface (by oversimplifying the velocity field and the geometry of the interface) and also underestimates the mixing of oxygen into the anoxic chimney (by neglecting molecular diffusion and mechanical dispersion). Because these two errors have opposing effects on the delivery of oxygen to the anoxic regions of the sediment (increasing it in the first instance and reducing it in the second instance), the net result is that the PASS and Kessler models yield similar estimates for the benthic flux of nitrate.

Collectively, these results suggest that the PASS model can be used in place of more numerically sophisticated models (such as Kessler's numerical flume model) for estimating nitrogen budgets and benthic fluxes in aquatic systems, while acknowledging that the fortuitous canceling of errors observed here may not apply in all cases. On the other hand, our COMSOL simulations (which are intermediate in sophistication and complexity between the PASS model and Kessler's numerical flume model) performed relatively poorly, and would not be suitable for estimating nitrate budgets in aquatic systems.

APPLICATION OF THE PASS MODEL TO SIX REPRESENTATIVE RIVERINE AND COASTAL MARINE SYSTEMS

Next we apply the PASS model to six aquatic environments where bedforms play an important role in nitrogen cycling. Three are rivers impacted by agriculture runoff, urban runoff, or sewage. The rest are marine systems with oligotrophic, low oxygen, or eutrophic bottom waters. Note that, for the marine settings, we assume that the ripples are formed by steady-state unidirectional currents (e.g., associated with persistent or tidal alongshore currents[41]) and not by shoaling waves. The latter are excluded because porewater flow induced by shoaling waves differs from that induced by unidirectional currents in a number of significant ways.[42]

We define the six environments by their "chemistry" (i.e., values of the seven nondimensional parameters in Table S1, columns 2 through 7) but leave their physical features (e.g., pore water flushing rate) as free variables. For each environment, we set out to answer the following questions: (1) How do physical features of a bedform influence nitrate removal? (2) What are the dominant biogeochemical pathways by which nitrate is generated and removed? (3) What is the relative contribution of direct denitrification and coupled nitrification—denitrification to overall nitrogen removal? (4) Are permeable sediments net sources or sinks of dissolved inorganic nitrogen?

To answer these questions, the PASS model was implemented in three steps. First, the "chemistry" of the six environments was established by selecting rate constants and in-stream oxygen and nutrient concentrations consistent with the literature[40,43−46] (columns 2 through 7, Table S1). Second, for each environment the rate equations (eqs S12a−S12c) were numerically integrated to yield the concentrations of oxygen, nitrate, and ammonium along any streamline through the sediment (Figure S2). Finally, the benthic flux of the ith species U_i (where the species of interest varied depending on the question being answered) was calculated as follows (derivation in the Supporting Information):
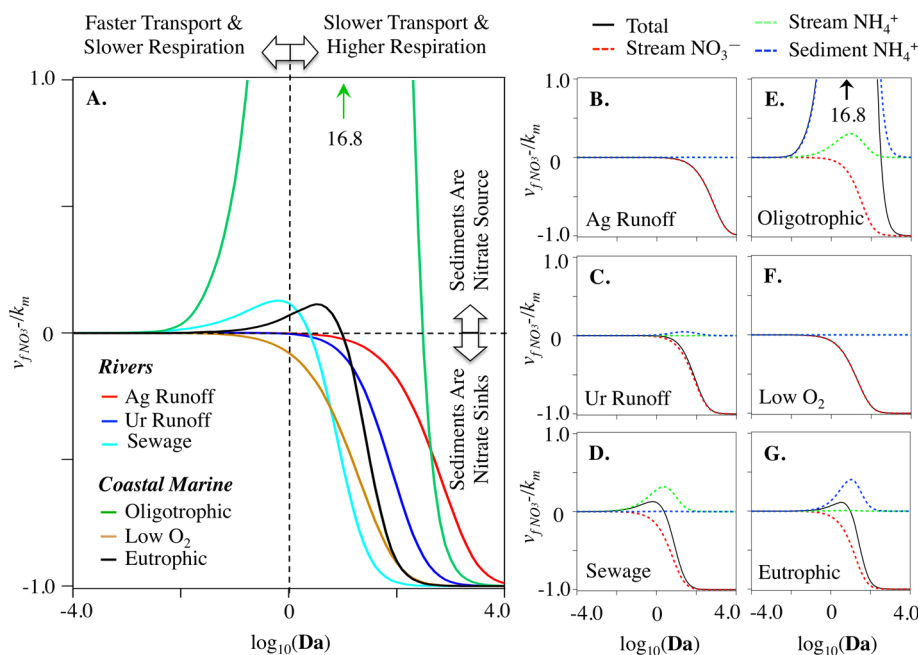
Figure 2. Application of the PASS model to six environments, including three rivers (impacted by agriculture runoff, urban runoff, or sewage) and three marine systems (with oligotrophic, low oxygen, or eutrophic bottom waters). The uptake velocity of nitrate ($v_{f\mathrm{NO_3}^-}$) depends on the pore-water flushing rate (k_m, both directly and through the definition of the Damkohler number) and environment-specific biogeochemical rate constants and in-stream concentrations of oxygen, nitrate, and ammonium (Table S1, Supplemental Information). The sign of the total uptake velocity indicates whether the streambed is a net source ($v_{f\mathrm{NO_3}^-} > 0$) or sink ($v_{f\mathrm{NO_3}^-} < 0$) of nitrate (A). The small panels show the contribution of different sources of nitrogen (including nitrate from the stream ("Stream NO_3^-"), ammonium from the stream ("Stream NH_4^+"), and ammonium generated in situ from the respiration of sediment organic matter ("Sediment NH_4^+")) to the uptake velocity of nitrate in three streams (agricultural runoff (B), urban runoff (C), and sewage (D)) and three marine systems (oligotrophic (E), low oxygen bottom water (F), and eutrophic (G)).

$$U_i = -k_m[C_i(0) - C_{i,\mathrm{bed}}] \tag{9a}$$

$$C_{i,\mathrm{bed}} = \int_{-\infty}^{\infty} C_i(\overline{\tau}_R = \mathbf{Da}\overline{\tau}_f; \text{ chemistry}) \frac{\mathrm{d}F_{\mathrm{RTD}}}{\mathrm{dlog}_{10}\,\overline{\tau}_f}\,\mathrm{dlog}_{10}\,\overline{\tau}_f \tag{9b}$$

Equation 9a is analogous to a film model for interfacial mass transfer in which the pore−water flushing rate k_m is equivalent to a mass transfer coefficient, $C_i(0)$ represents the in-stream concentration of the ith species entering the downwelling zone, and $C_{i,\mathrm{bed}}$ represents the RTD-weighted concentration of the ith species leaving the upwelling zone.[30] In the results shown below, we present benthic fluxes in terms of a so-called uptake velocity:[47] $v_i = U_i/C_{\mathrm{NO_3}^-}(0)$ where $C_{\mathrm{NO_3}^-}(0)$ is the nitrate concentration in the stream. Given our coordinate system, the sign of the uptake velocity indicates if bedforms are a net source ($v_i > 0$) or sink ($v_i < 0$) of the ith chemical species.

How do physical features of a bedform influence nitrate removal? Across all environments, the nitrate uptake velocity ($v_{f\mathrm{NO_3}^-} = U_{\mathrm{NO_3}^-}/C_{\mathrm{NO_3}^-}(0)$) depends on the pore water flushing rate, both directly and through the definition of the Damkohler Number (which depends on k_m through the transport time scale τ_T (see eq 1b)) (Figure 2A). Stream nitrate passes through the bedform without change when the Damkohler Number is small ($v_{f\mathrm{NO_3}^-}/k_m \rightarrow 0$, **Da** $< 10^{-2}$) and is completely removed when the Damkohler Number is large ($v_{f\mathrm{NO_3}^-}/k_m \rightarrow -1$, **Da** $> 10^3$). The limit $v_{f\mathrm{NO_3}^-}/k_m \rightarrow -1$ corresponds to the case where the removal of stream nitrate in the bedform is mass-transfer limited.[30] Between these two extremes, the magnitude and sign of the nitrate uptake velocity

varies by environment. In three environments (agriculture-impacted river, urban-impacted river, and low O_2 marine bottom water) the bedform is never a net source of nitrate ($v_{f\mathrm{NO_3}^-}/k_m < 0$, brown, dark blue, and red curves, Figure 2A). In the rest, bedforms are a net source of nitrate over some restricted range of the Damkohler number ($v_{f\mathrm{NO_3}^-}/k_m > 0$, green, light blue, and black curves, Figure 2A). In summary, the nitrate uptake velocity depends on sediment biogeochemistry ("**chemistry**"), the pore water flushing rate (k_m), and the balance between average respiration and transport rates in a bedform (as represented by the Damkohler number).

What Biogeochemical Pathways Dominate Nitrate Generation and Removal? To answer this question we evaluated the contribution of each nitrogen source to the nitrate uptake velocity (by integrating eqs (S17−S20), Supporting Information). In the two environments with limited nitrification (agriculture-impacted river and low-O_2 marine waters), the nitrate uptake velocity is determined solely by denitrification of stream nitrate (i.e., the red dashed and black curves overlap, Figure 2B,F). In the sewage-impacted river, the nitrate uptake velocity is the sum of uptake velocities associated with the oxidation of stream ammonium to nitrate and the reduction of stream nitrate to dinitrogen gas (i.e., the black curve is the sum of the red and green dashed curves, Figure 2D). In urban impacted rivers and eutrophic marine waters the nitrate uptake velocity has contributions from both the oxidation of sediment ammonium (generated by the respiration of sediment organic matter) and the reduction of stream nitrate (i.e., the black curve is the sum of the blue and red dashed curves, Figure 2C,G). Finally, in oligotrophic marine waters the nitrate uptake velocity has contributions from the reduction of
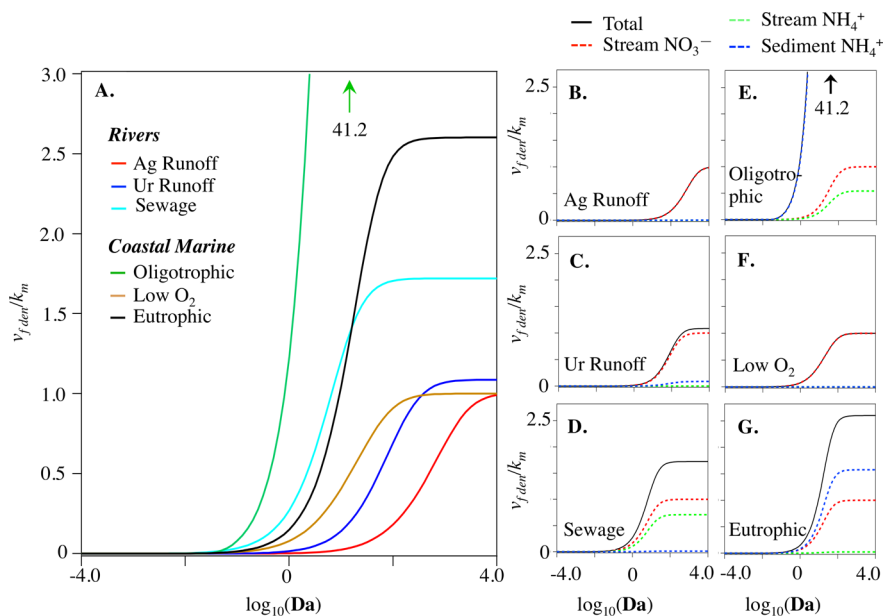
Figure 3. Same as Figure 2, except that the denitrification uptake velocity (v_{fden}) is plotted instead of total uptake velocity of nitrate ($v_{fNO_3^-}$).

stream nitrate, nitrification of sediment ammonium, and to a lesser extent nitrification of stream ammonium (i.e., the black curve is the sum of the dashed red, blue, and green curves, Figure 2E). The latter's large peak value ($v_{fNO_3^-}/k_m = 16.8$) can be attributed to conditions favorable for nitrification (oxygen saturated bottom waters) together with low nitrate concentrations in the overlying water column (recall that $v_{fNO_3^-}$ is the ratio of nitrate benthic flux and in-stream nitrate concentration).

What Is the Relative Importance of Direct Denitrification versus Coupled Nitrification−Denitrification? Nitrogen removal in bedforms can occur through direct denitrification (denitrification of stream nitrate) and/or coupled nitrification-denitrification (nitrification of stream and/or sediment ammonium followed by denitrification of the produced nitrate). To determine their relative importance, a denitrification velocity was calculated as follows:[47] $v_{fden} = 2U_{N_2}/C_{NO_3^-}(0)$, where the factor of 2 accounts for the fact that two molecules of nitrate are consumed for every one molecule of dinitrogen gas produced by denitrification. Because sediments can only be a source of N_2 (from denitrification) the denitrification velocity will always be positive ($v_{fden} > 0$). As illustrated in Figure 3A, the denitrification velocity depends sensitively on the Damkohler Number: small Damkohler Numbers are associated with low denitrification rates ($v_{fden} \rightarrow 0$ for $\mathbf{Da} < 1$), while large Damkohler Numbers are associated with high denitrification rates (i.e., v_{fden} approaches a fixed positive constant for $\mathbf{Da} > 10^2$). Consistent with the results presented by Zarnetske et al.,[38] the transition to net denitrification occurs around $\mathbf{Da} \approx 1$ (although the exact transition value for $\mathbf{Da}$ varies by environment, Figure 3A).

The relative importance of direct denitrification and coupled nitrification-denitrification can be ascertained from the limiting value of v_{fden}. When all stream nitrate entering a bedform is denitrified (and coupled nitrification-denitrification can be neglected), the flux of nitrate into the sediment bed is mass-transfer limited: $U_{NO_3^-} = -k_m C_{NO_3^-}(0)$. For every molecule of nitrate denitrified, one-half molecules of N_2 gas are formed.

Thus, the corresponding mass transfer-limited flux of nitrogen gas out of the sediment bed is $U_{N_2} = (k_m/2)C_{NO_3^-}(0)$. Substituting this last result into the definition of v_{fden} we arrive at the maximum denitrification velocity that can be achieved with direct-denitrification of stream nitrate alone: $v_{fden}/k_m \rightarrow 1.0$. This is precisely the limiting value observed in the two environments where nitrification rates are low (agricultural runoff and low-O_2 marine waters, red and brown curves, Figure 3A). In the other four environments the limiting value of v_{fden}/k_m exceeds unity, implying that at least some of the nitrogen loss can be attributed to coupled nitrification-denitrification (dark blue, light blue, black, and green curves, Figure 3A).

To obtain more detailed information on denitrification pathways, we evaluated the contribution of different nitrogen sources to the denitrification velocity. As expected, in the two environments with low nitrification rates (agricultural runoff and low-O_2 marine waters) all N_2 gas production can be attributed to direct denitrification of stream nitrate (i.e., the red dashed and black curves overlap, Figure 3B,F). In the remaining marine environments (oligotrophic and eutrophic), dinitrogen gas is formed from coupled nitrification−denitrification of sediment ammonium (produced from respiration of sediment organic material), direct denitrification of stream nitrate, and coupled nitrification-denitrification of stream ammonium (Figure 3E,G). Direct denitrification of stream nitrate dominates nitrogen removal in the urban runoff-impacted and sewage-impacted streams, with secondary contributions from coupled nitrification-denitrification of stream ammonium (sewage-impacted stream) or sediment ammonium (urban-impacted stream) (Figure 3C,D). In summary, under the right conditions, the PASS model suggests that coupled nitrification−denitrification can be an important pathway for nitrogen removal in bedforms, and even dominates in settings where stream nitrate concentrations are low (oliogotrophic and eutrophic marine waters). This conclusion—that coupled nitrification−denitrification dominates in sediments with low nitrate concentrations in the overlying water column—is consistent with field observations in lake, river, estuary, coastal, and continental shelf sediments.[48]

Are Bedforms Net Sources or Sinks of Dissolved Inorganic Nitrogen? To determine if bedforms generate more nitrate (by ammonification) than they remove (by dentrification) we calculated for each environment the dissolved inorganic nitrogen (DIN) uptake velocity: $v_{fDIN} = v_{fNO_3^-} + v_{fNH_4^+}$, where $v_{fNH_4^+} = U_{NH_4^+}/C_{NO_3^-}(0)$. In all cases, the DIN uptake velocity is greater than zero ($v_{fDIN} \geq 0$, Figure S8) implying that bedforms are a net source of DIN. It should be noted that the PASS model presented here assumes ammonification occurs at a constant rate throughout the sediment column (this was done so that we could directly compare PASS model results to the numerical flume results reported by Kessler, see earlier discussion). The sediments might have produced less DIN (and perhaps even been a net sink of DIN for some values of the Damkohler number) in the more realistic case where ammonification declines with depth.[40,43]

DEPENDENCE OF DENITRIFICATION VELOCITY ON IN-STREAM NITRATE CONCENTRATION

In a recent study of nitrogen cycling in 49 streams across the U.S., Mulholland et al.[49] reported that the denitrification velocity declines as a power-law of in-stream nitrate concentration:

$$v_{fden} = 0.001 \times C_{NO_3^-}(0)^{-b}, \quad b = 0.5 \tag{10}$$

This finding is significant because it implies a stream's ability to process and remove nitrate (an important ecosystem service) is diminished as the nitrate concentration in a stream increases (e.g., due to increased loading of nitrate from agricultural runoff). Provided that nitrification and oxygen inhibition of denitrification are negligible, two exact solutions for v_{fden} can be derived from the PASS model in the limits where in-stream nitrate concentration is much larger or smaller than the half-saturation constant for denitrification (derivation in the Supporting Information):

$$v_{fden} = k_m G\left(\frac{\mathbf{Da}\kappa K_{O_2}^{sat}}{K_{NO_3^-}^{sat}}\right) \propto C_{NO_3^-}(0)^0, \quad C_{NO_3^-}(0) \ll K_{NO_3^-}^{sat} \tag{11a}$$

$$v_{fden} = \frac{57.6 k_m \mathbf{Da}\kappa K_{O_2}^{sat}}{C_{NO_3^-}(0)} \propto C_{NO_3^-}(0)^{-1}, \quad C_{NO_3^-}(0) \gg K_{NO_3^-}^{sat} \tag{11b}$$

The function $G(v)$ appearing in eq 11a is an integral expression that can be evaluated numerically for any choice of the independent variable $v = \mathbf{Da}\kappa K_{O_2}^{sat}/K_{NO_3^-}^{sat}$ (see the Supporting Information). These two limits imply that denitrification velocity will decline with increasing in-stream nitrate concentration (consistent with Mulholland's empirical correlation). However, instead of a single-power-law exponent b (as in eq 10), the PASS model predicts that the power-law exponent transitions from $b = 0$ to $b = 1$ in the limit of large in-stream nitrate concentration. These two exponent limits bracket error bounds for Mulholland's single power-law exponent (95% and 5% confidence values of $b = 0.2$ and 0.7, respectively) computed using nonparametric bootstrap techniques (see the Supporting Information). Thus, our PASS model predictions are consistent with Mulholland's empirical correlation, at least within the scatter of Mulholland's data set

and the assumptions employed to derive eqs 11a and 11b. Importantly, the PASS model provides a mechanism for Mulholland's observation that v_{fden} declines with $C_{NO_3^-}(0)$: the change in exponent value corresponds to a transition in the denitrification rate from first-order at low nitrate concentrations ($C_{NO_3^-}(0) \ll K_{NO_3^-}^{sat}$, $b = 0$) to zero-order at high nitrate concentrations ($C_{NO_3^-}(0) \gg K_{NO_3^-}^{sat}$, $b = 1$) (see eq 6d). Indeed, the in-stream nitrate concentrations reported by Mulholland (average 0.04 mol m^{-3}, range 0– 1.51 mol m^{-3}) straddle values of $K_{NO_3^-}^{sat}$ values adopted earlier for sewage-, agricultural-, and urban- impacted streams (0.002, 0.01, and 0.02 mol m^{-3}, see Table S1). Thus, both first-order and zero-order denitrification kinetics were likely represented in the streams Mulholland selected for their study.

As noted by Mulholland et al.,[49] the fraction $f_{NO_3^-}$ of nitrate mass loading removed over a stream reach can be calculated from the nitrate uptake velocity v_f, the volumetric flow rate Q, and sediment bed surface area SA: $f_{NO_3^-} = 1 - e^{-v_f \, SA/Q}$. The degree to which a stream network removes nitrate from the terrestrial landscape will therefore depend on the topology of the stream network (i.e., how the stream reaches are organized within the watershed) as well as hydraulic and chemical features of the stream that affect v_f (the focus of the present paper). It remains an open question how these three factors—stream topology, hydraulics, and chemistry—collectively influence the removal of nitrate in natural and urban catchments. Mulholland et al. also noted that a significant fraction of stream nitrate uptake was associated with storage in the sediment bed, either in the form of biomass or particulate material. Incorporating kinetics for nitrate storage into the PASS model is therefore an obvious target for future research.

MODEL LIMITATIONS AND FUTURE DIRECTIONS

Beyond the limitations already noted, the PASS model does not account for a number of processes known to affect nitrogen budgets in aquatic systems. We plan to address three such limitations in future evolutions of the model: (1) influence of flow fields operating over different scales (e.g., bedform exchange coupled with regional upwelling of groundwater); (2) formation of redox microzones in heterogeneous sediments; and (3) spatially variable patterns of organic carbon and respiration rates. First, Boano and co-workers demonstrated that the superposition of groundwater-stream interactions (e.g., associated with gaining or losing streams) alters the RTD of bedform exchange, in part by limiting the depth over which bedform exchange can occur.[50,51] Thus, upwelling groundwater, for example, could affect nitrate concentrations in rivers both directly by adding nitrate (if the groundwater is contaminated with nitrate) and indirectly by altering the biogeochemical transformations that depend on the RTD of water parcels in the sediment (note that nitrate flux into the sediment depends explicitly on the RTD, see eq 9b). Second, bedforms are heterogeneous with respect to sediment grain sizes[52] and flowpaths.[53,54] This heterogeneity can lead to mixing across streamlines[55,56] and facilitate the formation of redox microzones (e.g., localized pockets of denitrification embedded within well-oxygenated downwelling regions) that enhance coupled nitrification-denitrification and overall nitrate removal rates in natural sediments.[36,55] Third, organic carbon and microbial respiration rates are spatially variable, not homogeneous as assumed in the present modeling effort. For example,

bulk organic carbon concentration often declines with depth into the sediment bed[57] and/or can be locally concentrated, for example, in the form of buried fecal pellets.[58]

■ ASSOCIATED CONTENT

⑤ Supporting Information

The Supporting Information is available free of charge on the ACS Publications website at DOI: 10.1021/acs.est.5b01941.

> Mathematical derivations, bootstrap analysis, figures, tables, and experimental data (PDF)

■ AUTHOR INFORMATION

Corresponding Author

*E-mail: sbgrant@uci.edu. Tel: (949) 824-8277. Fax: (949) 824-2541.

Notes

The authors declare no competing financial interest.

■ ACKNOWLEDGMENTS

■ REFERENCES

(1) Hall, S. J. The Continental Shelf Benthic Ecosystem: Current Status, Agents for Change and Future Prospects. *Environ. Conserv.* **2002**, *29*, 350−374.

(2) Brunke, M.; Gonser, T. The Ecological Significance of Exchange Processes between Rivers and Groundwater. *Freshwater Biol.* **1997**, *37*, 1−33.

(3) Young, B. a.; Norris, R. H.; Sheldon, F. Is the Hyporheic Zone a Refuge for Macroinvertebrates in Drying Perennial Streams? *Mar. Freshwater Res.* **2011**, *62*, 1373−1382.

(4) Gandy, C. J.; Smith, J. W. N.; Jarvis, A. P. Attenuation of Mining-Derived Pollutants in the Hyporheic Zone: A Review. *Sci. Total Environ.* **2007**, *373*, 435−446.

(5) Lawrence, J. E.; Skold, M. E.; Hussain, F. A.; Silverman, D. R.; Resh, V. H.; Sedlak, D. L.; Luthy, R. G.; McCray, J. E. Hyporheic Zone in Urban Streams: A Review and Opportunities for Enhancing Water Quality and Improving Aquatic Habitat by Active Management. *Environ. Eng. Sci.* **2013**, *30*, 480−501.

(6) Cook, P.; Wenzhöfer, F.; Rysgaard, S.; Galaktionov, O. S.; Meysman, F. J. R.; Eyre, B. D.; Cornwell, J.; Huettel, M.; Glud, R. N. Quantification of Denitrification in Permeable Sediments: Insights from a Two-Dimensional Simulation Analysis and Experimental Data. *Limnol. Oceanogr.: Methods* **2006**, *4*, 294−307.

(7) Pinay, G.; O'Keefe, T. C.; Edwards, R. T.; Naiman, R. J. Nitrate Removal in the Hyporheic Zone of a Salmon River in Alaska. *River Res. Appl.* **2009**, *25*, 367−375.

(8) Bardini, L.; Boano, F.; Cardenas, M. B.; Revelli, R.; Ridolfi, L. Nutrient Cycling in Bedform Induced Hyporheic Zones. *Geochim. Cosmochim. Acta* **2012**, *84*, 47−61.

(9) Huettel, M.; Berg, P.; Kostka, J. E. Benthic Exchange and Biogeochemical Cycling in Permeable Sediments. *Annu. Rev. Mar. Sci.* **2014**, *6*, 23−51.

(10) Howarth, R.; Sharpley, A.; Walker, D. Sources of Nutrient Pollution to Coastal Waters in the United States: Implications for Achieving Coastal Water Quality Goals. *Estuaries* **2002**, *25*, 656−676.

(11) David, M.; Wall, L.; Royer, T.; Tank, J. Denitrification and the Nitrogen Budget of a Reservoir in an Agricultural Landscape. *Ecol. Appl.* **2006**, *16*, 2177−2190.

(12) Galloway, J. N.; et al. Nitrogen Cycles: Past, Present, and Future. *Biogeochemistry* **2004**, *70*, 153−226.

(13) David, A.; Perrin, J. L.; Rosain, D.; Rodier, C.; Picot, B.; Tournoud, M. G. Implications of Two In-Stream Processes in the Fate of Nutrients Discharged by Sewage Systems into a Temporary River. *Environ. Monit. Assess.* **2011**, *181*, 491−507.

(14) Haggard, B. E.; Stanley, E. H.; Storm, D. E. Nutrient Retention in a Point-Source-Enriched Stream. *J. N. Am. Benthol. Soc.* **2005**, *24*, 29−47.

(15) Grant, S. B.; Litton-Mueller, R. M.; Ahn, J. H. Measuring and Modeling the Flux of Fecal Bacteria across the Sediment-Water Interface in a Turbulent Stream. *Water Resour. Res.* **2011**, *47*, W05517.

(16) Litton, R. M.; Ahn, J. H.; Sercu, B.; Holden, P. A.; Sedlak, D. L.; Grant, S. B. Evaluation of Chemical, Molecular, and Traditional markers of Fecal Contaminantion in an Effluent Dominated Urban Stream. *Environ. Sci. Technol.* **2010**, *44*, 7369−7375.

(17) Sinigalliano, C. D.; Gidley, M. L.; Shibata, T.; Whitman, D.; et al. Impacts of Hurricanes Katrina and Rita on the Microbial Landscape of the New Orleans Area. *Proc. Natl. Acad. Sci. U. S. A.* **2007**, *104*, 9029−9034.

(18) Searcy, E.; Packman, A. I.; Atwill, E. R.; Harter, T. Deposition of *Cryptosporidium* Oocysts in Streambeds. *Appl. Environ. Microbiol.* **2006**, *72*, 1810−1816.

(19) Boano, F.; Harvey, J.; Marion, A.; Packman, A. I.; Revelli, R.; Ridolfi, L.; Worman, A. Hyporheic Flow and Transport Processes: Mechanisms, Models, and Biogeochemical Implications. *Rev. Geophys.* **2014**, *52*, 603.

(20) Meysman, F. J. R.; Galaktionov, O. S.; Cook, P. L. M.; Janssen, F.; Huettel, M.; Middelburg, J. J. Quantifying Biologically and Physically Induced Flow and Tracer Dynamics in Permeable Sediments. *Biogeosciences* **2007**, *4*, 627−646.

(21) Santos, I. R.; Eyre, B. D.; Huettel, M. The Driving Forces of Porewater and Groundwater Flow in Permeable Coastal Sediments: A Review. *Estuarine, Coastal Shelf Sci.* **2012**, *98*, 1−15.

(22) Hester, E. T.; Gooseff, M. N. Moving beyond the banks: hyporheic restoration is fundamental to restoring ecological services and functions of streams. *Environ. Sci. Technol.* **2010**, *44*, 1521−1525.

(23) Stonedahl, S. H.; Harvey, J. W.; Wörman, A.; Salehin, M.; Packman, A. I. A Multiscale Model for Integrating Hyporheic Exchange from Ripples to Meanders. *Water Resour. Res.* **2010**, *46*, W12539.

(24) Stonedahl, S. H.; Harvey, J. W.; Detty, J.; Aubeneau, A.; Packman, A. I. Physical Controls and Predictability of Stream Hyporheic Flow Evaluated with a Multiscale Model. *Water Resour. Res.* **2012**, *48*, W10513.

(25) Grant, S. B.; Marusic, I. Crossing Turbulent Boundaries: Interfacial Flux in Environmental Flows. *Environ. Sci. Technol.* **2011**, *45*, 7107−7113.

(26) Elliott, A. H.; Brooks, N. H. Transfer of Nonsorbing Solutes to a Streambed with Bed Forms: Laboratory Experiments. *Water Resour. Res.* **1997**, *33*, 137−151.

(27) Elliott, A. H.; Brooks, N. H. Transfer of Nonsorbing Solutes to a Streambed with Bed Forms: Theory. *Water Resour. Res.* **1997**, *33*, 123−136.

(28) Cardenas, M. B.; Wilson, J. L. Dunes, Turbulent Eddies, and Interfacial Exchange with Permeable Sediments. *Water Resour. Res.* **2007**, *43*, W08412.

(29) Janssen, F.; Cardenas, M. B.; Sawyer, A. H.; Dammrich, T.; Krietsch, J.; de Beer, D. A comparative experimental and multiphysics computational fluid dynamics study of coupled surface-subsurface flow in bedforms. *Water Resour. Res.* **2012**, *48*, W08514.

(30) Grant, S. B.; Stolzenbach, K.; Azizian, M.; Stewardson, M. J.; Boano, F.; Bardini, L. First-Order Contaminant Removal in the Hyporheic Zone of Streams: Physical Insights from a Simple Analytical Model. *Environ. Sci. Technol.* **2014**, *48*, 11369−11378.

(31) Levenspiel, O. *Chemical Reaction Engineering*; Wiley: New York, 1972.

(32) Rutherford, J. C.; Boyle, J. D.; Elliott, A. H.; Hatherell, T. V. J.; Chiu, T. W. Modeling benthic oxygen uptake by pumping. *J. Environ. Eng.* **1995**, *121*, 84−95.

(33) Berg, P.; Long, M. H.; Huettel, M.; Rheuban, J. E.; McGlathery, K. J.; Howarth, R. W.; Foreman, K. H.; Giblin, A. E.; Marino, R. Eddy Correlation Measurements of Oxygen Fluxes in Permeable Sediments Exposed to Varying Current Flow and Light. *Linol. Oceangr.* **2013**, *58*, 1329−1343.

(34) *A model set-up for an oxygen and nutrient flux model for Aarhus Bay (Denmark)*; NERI Technical Report No. 483; National Environmental Research Institute, Roskilde, Denmark, 2004.

(35) Hill, C. G. *An introduction to chemical engineering kinetics and reactor design*; John Wiley and Sons: New York, 1977; Chapter 11.

(36) Briggs, M. A.; Day-Lewis, F. D.; Arnteske, J. P.; Harvey, J. W. A physical explanation for the development of redox microzones in hyporheic flow. *Geophys. Res. Lett.* **2015**, *42*, doi:440210.1002/2015GL064200.

(37) Marzadri, A.; Tonina, D.; Bellin, A. A Semianalytical Three-Dimensional Process-Based Model for Hyporheic Nitrogen Dynamics in Gravel Bed Rivers. *Water Resour. Res.* **2011**, *47*, W11518.

(38) Zarnetske, J. P.; Haggerty, R.; Wondzell, S. M.; Bokil, V. A.; Gonzalez-Pinzon, R. Coupled transport and reaction kinetics control the nitrate source-sink function of hyporheic zones. *Water Resour. Res.* **2012**, *48*, W11508.

(39) Kessler, A. J.; Glud, R. N.; Cardenas, M. B.; Cook, P. L. M. Transport Zonation Limits Coupled Nitrification-Denitrification in Permeable Sediments. *Environ. Sci. Technol.* **2013**, *47*, 13404−13411.

(40) Kessler, A. J.; Glud, R. N.; Cardenas, M. B.; Larsen, M.; Bourke, M. F.; Cook, P. L. M. Quantifying Denitrification in Rippled Permeable Sands through Combined Flume Experiments and Modeling. *Limnol. Oceanogr.* **2012**, *57*, 1217−1232.

(41) Fischer, H.; List, J.; Koh, C.; Imberger, J.; Brooks, N. *Mixing in inland and coastal waters*; Academic Press: New Yor, 1979.

(42) Cardenas, M. B.; Jiang, H. Wave-driven porewater and solute circulation through rippled elastic sediment under highly transient forcing. *Limon. Oceanog.: Fluids and Environments* **2011**, *1*, 23−37.

(43) Evrard, V.; Glud, R. N.; Cook, P. L. M. The kinetics of denitrification in permeable sediments. *Biogeochemistry* **2013**, *113*, 563−572.

(44) Marchant, H. K.; Lavik, G.; Holtappels, M.; Kuypers, M. M. M. *PLoS One* **2014**, *9*, e104517.

(45) Potter, J. D.; McDowell, W. H.; Helton, A. M.; Daley, M. L. Incorporating urban infrastructure into biogeochemical assessment of urban tropical streams in Puerto Rico. *Biogeochemistry* **2014**, *121*, 271−286.

(46) Howarth, R. W.; et al. Regional Nitrogen Budgets and Riverine N and P Fluxes for the Drainages to the North Atlantic Ocean: Natural and Human Influences. *Biogeochemistry* **1996**, *35*, 75−139.

(47) Stream Solute Workshop.. Concepts and Methods for Assessing Solute Dynamics in Stream Ecosystem. *J. N. Am. Benthol. Soc.* **1990**, *9*, 95−119.

(48) Seitzinger, S.; Harrison, J. A.; Bohlke, J. K.; Bouwman, A. F.; Lowrance, R.; Peterson, B.; Tobias, C.; Van Drecht, G. Denitrification across landscapes and waterscapes: a synthesis. *Ecological Applications* **2006**, *16* (6), 2064−2090.

(49) Mulholland, P. J.; et al. Stream denitrification across biomes and its response to anthropogenic nitrate loading. *Nature* **2008**, *452*, 202−205.

(50) Boano, F.; Revelli, R.; Ridolfi, L. Reduction of the hyporheic zone volume due to the stream-aquifer interaction. *Geophys. Res. Lett.* **2008**, *35*, L09401.

(51) Boano, F.; Revelli, R.; Ridolfi, L. Quantifying the impact of groundwater discharge on the surface-subsurface exchange. *Hydrol. Processes* **2009**, *23*, 2108−2116.

(52) Cardenas, M. B.; Wilson, J. L.; Zlotnik, V. A. Impact of heterogeneity, bed forms, and stream curvature on subchannel hyporheic exchange. *Water Resour. Res.* **2004**, *40*, W08307.

(53) Menichino, G. T.; Ward, A. S.; Hester, E. T. Macropores as preferential flow paths in meander bends. *Hydrol. Process.* **2014**, *28*, 482−495.

(54) Menichino, G. T.; Scott, D. T.; Hester, E. T. abundance and dimensions of naturally occuring macropores along stream channels and the effects of artificially constructed large macropores on transient storage. *Freshwater Science* **2015**, *34*, 125−138.

(55) Sawyer, A. H. Enhanced removal of groundwater-borne nitrate in heterogeneous aquatic sediments. *Geophys. Res. Lett.* **2015**, *42*, 403−410.

(56) Triska, F. J.; Kennedy, V. C.; Avanzino, R. J.; Zellweger, G. W.; Bencala, K. E. Retention and transport of nutrients in a third-order stream in northwestern California: Hyporheic processes. *Ecology* **1989**, *70* (6), 1893−1905.

(57) Cook, P. L.; et al. Quantification of denitrification in permeable sediments: insights from a two-dimensional simulation analysis and experimental data. *Limnol. Oceanogr.: Methods* **2006**, *4*, 294−307.

(58) Jørgensen, B. B. Bacterial sulfate reduction within reduced microniches of oxidized marine sediments. *Mar. Biol.* **1977**, *41* (1), 7−17.